Accepted Manuscript

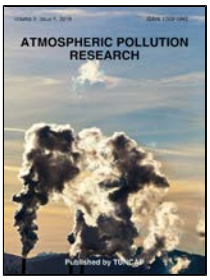

Airborne concentration and deposition of trace metals and metalloids in an urban area downwind of a manganese alloy plant

A. Hernández-Pellón, I. Fernández-Olmo

PII:	S1309-1042(18)30548-8
DOI:	10.1016/j.apr.2018.11.009
Reference:	APR 471
To appear in:	*Atmospheric Pollution Research*
Received Date:	17 September 2018
Accepted Date:	19 November 2018

Please cite this article as: A. Hernández-Pellón, I. Fernández-Olmo, Airborne concentration and deposition of trace metals and metalloids in an urban area downwind of a manganese alloy plant, *Atmospheric Pollution Research* (2018), doi: 10.1016/j.apr.2018.11.009

Airborne concentration and deposition of trace metals and metalloids in an urban area downwind of a manganese alloy plant

A. Hernández-Pellón[a*] and I. Fernández-Olmo[a]

[a] Dpto. de Ingenierías Química y Biomolecular, Universidad de Cantabria, Avda. Los Castros s/n, 39005 Santander, Cantabria, Spain

*Corresponding author
Dpto. de Ingenierías Química y Biomolecular, Universidad de Cantabria, Avda. Los Castros s/n, 39005 Santander, Cantabria, Spain
ana.hernandez@unican.es

Abstract

The evaluation of the content of metals and metalloids in particulate matter (PM) and in atmospheric deposition in areas impacted by local industries is essential from an environmental and health risk perspective. In this study, the PM_{10} levels and atmospheric deposition fluxes of potentially toxic metals and metalloids were quantified at three urban sites of the Cantabrian region (northern Spain), located at different distances downwind of a Mn alloy plant. The content of Mn, V, Fe, Ni, Cu, Zn, As, Mo, Cd, Sb and Pb in PM_{10} and in the water-soluble and insoluble fractions of the deposition was determined by ICP-MS. Among the studied elements, the highest concentrations in PM_{10} and deposition rates were found for Mn, Fe, Zn and Pb, associated with the Mn alloy industry, and for Cu, related to non-exhaust traffic emissions. The levels of Mn, Fe, Zn and Pb in PM_{10} were higher in autumn, when the most frequent winds blow from the S-SW, whereas their highest deposition rates were found in winter and autumn, which are characterized by high monthly average precipitations. The water-soluble fraction of the atmospheric deposition of most metals increased with distance from the Mn alloy plant. The highest water-soluble fractions were found for Ni (72%), Zn (62%), Cu (60%) and Mn (49%). These results will be useful for the health risk assessment of the metal exposure associated with Mn alloy plants, as well as for the evaluation of the metal burden to soil, water and ecosystems related to this industrial activity.

Keywords

PM_{10}, Bulk atmospheric deposition, Water-soluble fraction; Manganese alloy plant, Metal; Metalloid

1. Introduction

Atmospheric pollution is a significant cause of concern worldwide. Particulate matter (PM) exposure is associated with an extensive number of cardiovascular, respiratory and neurological diseases (Davidson et al., 2005; Fiordelisi et al., 2017; Hoek et al., 2013; Raaschou-Nielsen et al., 2013; Wang et al., 2017); PM is also considered as carcinogenic to humans (Group 1) by the International Agency for Research on Cancer (IARC) (IARC, 2016).

The aerosol toxicity is strongly linked to the physico-chemical characteristics of particles (i.e. size, morphology and chemical composition), which vary according to the different emission sources (Kelly and Fussell, 2012). In this regard, the metal and metalloid content of PM is of special interest in urban and industrial areas, where non-exhaust traffic emissions (Amato et al., 2014; Thorpe and Harrison, 2008), oil/fuel combustion (Bourliva et al., 2018; Fomba et al., 2018) and industrial activities such as the steel or the ferroalloy production (Lucas et al., 2015; Mbengue et al., 2017; Sylvestre et al., 2017) are considered the main metal and metalloid sources (e.g. iron (Fe), zinc (Zn), lead (Pb), manganese (Mn)). Metal-bearing particles can be transported long distances from the emission source depending on the height of the point sources, the meteorological conditions and the physicochemical characteristics of the particles (Connan et al., 2013; Omrani et al., 2017). Studies related to the levels of metals and metalloids in PM in urban and industrial areas, in combination with some physico-chemical characteristics (e.g. segregation by particle size or solubility) are commonly found in the literature (Coufalík et al., 2016; Fomba et al., 2018; Hernández-Pellón et al., 2017; Mbengue et al., 2017). The airborne levels of such elements are not only dependent on their emission rates and atmospheric dispersion mechanisms, but also on their removal rate from the atmosphere.

The main mechanisms for the removal of PM and its components are scavenging (wet deposition) and dry deposition (Connan et al., 2013). Although wet deposition is considered an important process for PM removal, in regions with low precipitation, such as the Mediterranean climate area, dry deposition is more important than wet deposition on an annual basis (Pan and Wang, 2015). However, since the relative contribution of both mechanisms highly depends on the local meteorological conditions, a suitable assessment of the atmospheric deposition should include both dry and wet deposition.

Despite the cleaning effect of both mechanisms in the atmosphere, deposition is also implicated in the transfer of metals and metalloids from air to aquatic (Child et al., 2018; Engels et al., 2018; Lintern et al., 2016) and terrestrial ecosystems (Borgese et al., 2013; Carter et al., 2015; Hovmand et al., 2008; Pavilonis et al., 2016), and, subsequently, to the food chain (Antisari et al., 2015; Bermudez et al., 2012; Folens et al., 2017). In addition, deposited PM also contributes to air pollution through the mechanism of resuspension (Castillo et al., 2013a; Pant and Harrison, 2013). Therefore, the study of the atmospheric deposition is important not only as a mechanism for pollutant removal and transport, and as a measure of the pollutant burden to soil, water and ecosystems, but also from a health risk perspective (Taylor, 2015).

The dry and wet deposition of metals and metalloids may be estimated by using bulk (funnel/bottle) or Bergerhoff (bucket) collectors, whereas wet deposition is usually determined by wet-only collectors (funnel/bottle) (Amodio et al., 2014). The use of Bergerhoff and bulk collectors is recommended at industrial and very dry urban and rural areas (Aas et al., 2009). Additionally, several authors have reported the limitations in relation with the measurement of dry deposition in urban areas, without taking into account the variety of urban surfaces (i.e. glass, tile, grass, etc.) (Omrani et al., 2017; Percot et al., 2016; Roupsard et al., 2013).

Numerous research studies have determined the levels of metals and metalloids in atmospheric deposition in rural (Connan et al., 2013; Hovmand et al., 2008; Tositti et al., 2018) and urban areas (Davis and Birch, 2011; Guo et al., 2017; Liang et al., 2016; Norouzi et al., 2017; Omrani et al., 2017) around the world. Other studies focused on the assessment of metal and metalloid deposition in areas located close to specific anthropogenic activities, such as road traffic (Al Ali et al., 2017; Aljazzar and Kocher, 2016), port operations (Castillo et al., 2013b; Taylor, 2015), and industrial activities such as the steel-making industry (Amodio et al., 2014), copper (Cu) smelters (Fedorová et al., 2015), Pb smelters (Qiu et al., 2016), Fe ore works (Hančuľák et al., 2011), mining (Castillo et al., 2013a; Marrugo-Negrete et al., 2014), glass making plants (Rossini et al., 2010) or municipal solid waste incinerators (MSWI) (Venturini et al., 2013). Only a few studies deal with the metal and metalloid deposition in the vicinity of Mn alloy plants, mainly focused on the assessment of the Mn content in soils or cultivated vegetables (Boudissa et al., 2006; Ferri et al., 2015), household dust (Lucas et al., 2015), or on the estimation of Mn deposition by dispersion modeling and its relation with its content in

local soils (Carter et al., 2015). Only Menezes-Filho et al. (2016) deal with the Mn and Pb accumulation in dust fall in exterior environments at different distances from a Mn alloy plant.

This study aims to deepen into the impacts of Mn alloy plants on the levels of nine metals (i.e. Mn, Fe, Cu, Zn, Pb, vanadium (V), nickel (Ni), molybdenum (Mo) and cadmium (Cd)) and two metalloids (i.e. arsenic (As) and antimony (Sb)) in air, as well as on the potential transfer of these pollutants to aquatic or terrestrial ecosystems by atmospheric deposition. The PM_{10} levels and the deposition fluxes (water-soluble and insoluble fraction) of these metals and metalloids were quantified at three different distances downwind of a Mn alloy plant, which correspond to three urban sites of the Cantabrian region (northern Spain). This area is of special interest due to the fact that more than 250,000 people live at less than 10 km from the Mn alloy plant. The comparison between the sampling sites, the seasonal variability of the content of metals and metalloids in PM_{10} and in atmospheric deposition, as well as the variability of the metal and metalloid water-soluble fractions with distance from the Mn alloy plant were investigated.

2. Materials and methods

2.1 Area of study

The area of study of this work is located in the north of Spain, in the region of Cantabria (580,140 inhabitants, 2017), specifically along the Santander Bay. This study has been conducted in the following locations:

1) Santander (171,951 inhabitants, 2017), which is placed in the northern part of the Santander Bay, is the most populated city of the region and is mainly focused on residential and commercial activities. The ETSIIT site (UTM, 30T, X=435450, Y=4813651, 7 m a.s.l.) is situated on the campus of the University of Cantabria, on the rooftop of the "E.T.S de Ingenieros Industriales y de Telecomunicaciones "building (30 m above ground) and represents an urban background site.
2) Maliaño (9492 inhabitants, 2017), is a town located in the southern part of the Santander Bay. This urban area, where a Mn alloy plant is located, is characterized by high concentrations of Mn in air, according to the WHO criteria (Hernández-Pellón et al., 2017). A sampling site was selected in the town center: the CROS

site (UTM, 30T, X=431916, Y=4807982, 6 m a.s.l.), which is an official monitoring station that belongs to the Cantabrian Regional Government. This site is located 850 m from the Mn alloy plant and represents an urban/industrial mixed area. Additionally, a second sampling point was selected in the urban area located closest to the Mn alloy plant, the CCV site (UTM, 30T, X=431899, Y=4807290, 5 m a.s.l.); the sampler was placed on the rooftop of the "Cultural Center of La Vidriera". This site is located only 350 m from the Mn alloy plant.

The location of the sampling sites and the main metal and metalloid sources is shown in Figure 1. In addition, Figure 2 shows the wind roses for the sampling periods at the three sampling sites. As can be seen, the most frequent winds came from the S-SW during the PM_{10} and atmospheric deposition sampling campaigns (see below section), in agreement with the prevailing wind directions of the region. A lower contribution of NNE winds is also observed in Figure 2; this wind sector is only characteristic of the warm period in the Santander Bay (Moreno et al., 2011). So, according to the wind roses shown in Figure 2, the three sampling sites are located downwind of the Mn alloy plant most of the sampling period, and therefore this allows us to study the influence of the distance from the main sources on the concentration and deposition of the studied metals and metalloids.

2.2 PM_{10} and bulk deposition sampling

A simultaneous PM_{10} and bulk atmospheric deposition sampling campaign was conducted from January 2015 to January 2016 at the CROS and the ETSIIT sites. PM_{10} samples were collected weekly by a high volume sampler device (30 m^3/h, MCV) on 150 mm quartz fiber filters (Sartorious). Overall, 52 and 55 daily samples were taken at the CROS and the ETSIIT sites, respectively. Bulk atmospheric deposition was collected using a bulk bottle/funnel sampler based on the European standard UNE-EN 15841:2010, "Standard method for determination of As, Cd, Pb and Ni in atmospheric deposition". The collector consisted of a polyethylene bottle connected to a funnel with a 0.078 m^2 collection area. The funnel was at 1.7 m above the ground to avoid the collection of re-suspended dust and the collector was placed on a steel chassis with a protective ring to avoid bird nesting. Bulk deposition sampling periods were 30±3 days. A total of 12 samples were collected at each monitoring site during the whole campaign. At the end of each sampling period, the inner surface of the funnel was washed with 250 ml of Milli-Q water and the funnel and plastic bottle were replaced by a clean one.

As indicated in section 2.1, an additional bulk atmospheric deposition sampling campaign was performed later at the CCV site; the sampling period was from September 2015 to December 2016. A total of 12 monthly samples were collected during this campaign. Due to operational limitations at the CCV site, PM_{10} samples were only taken in September 2015. A total of 28 daily samples were collected on 47 mm quartz fiber filters (Sartorius) using a low volume sampler device (2.3 $m^3 \cdot h^{-1}$).

2.3 Sample preparation and metal analysis

Upon bulk deposition sampling, a gravimetric determination of the total precipitation was performed by a top loading balance (Sartorius, M-pact AX4202). Acidity was measured in 50 ml of the unfiltered sample using a portable pH meter (Crison, pH-25). Then, the water-soluble and insoluble fractions were separated by filtering the samples through 0.45 µm nitrocellulose filters (47 mm, Merck). An aliquot of the water-soluble fraction (50 ml) was acidified with HNO_3 and stored refrigerated (4ºC) until future use.

The total content of metals and metalloids in PM_{10} and in the water-insoluble fraction of the atmospheric deposition was determined based on the European standard method EN-UNE 14902:2006 "Standard method for the measurements of Pb, Cd, As and Ni in the PM_{10} fraction of suspended particulate matter". The acid digestion of the filters (i.e. the PM_{10} samples and the water-insoluble deposition samples) was performed in a microwave digestion system (Milestone, Ethos One, Italy) using closed Teflon vessels (HNO_3:H_2O_2 8:2, up to 220 ºC). The reagents used were of high purity (Suprapur®, Merck). The content of V, Mn, Fe, Ni, Cu, Zn, As, Mo, Cd, Sb and Pb in the extracts of the insoluble fraction of bulk atmospheric deposition and PM_{10} samples as well as in the water-soluble fraction of the deposition samples was analyzed by inductively coupled plasma mass spectrometry (ICP-MS, Agilent 7500 CE). The operating conditions are shown in Table 1. Quality control of the analytical procedure included the determination of the recovery values of the analyzed metals and metalloids from a standard reference material (NIST SRM 1648a, "Urban particulate matter"), as well as the evaluation of the blank contribution from the filters and reagents and subsequent subtraction from the results. Recovery values and method detection limits (MDL) of the mentioned metals and metalloids are shown in Table 2. Concentrations were reported as $ng \cdot m^{-3}$ for PM_{10} samples, whereas bulk atmospheric deposition fluxes were expressed as $\mu g \cdot m^{-2} \cdot d^{-1}$

2.4 Data analysis

Statistical analysis of the data was performed using R statistical software version 3.3.0. All data distributions were checked for normality using the Shapiro-Wilks test. This test was selected due to the small size of the datasets. Since most distributions deviated from the normality, the relationship between total metal and metalloid concentrations in PM_{10} and also in bulk atmospheric deposition at each studied site was evaluated by determining the Spearman correlation coefficients. As the pairwise correlation involves multiple comparisons, the "Holm test" (Holm, 1979) was used to adjust the p-values to count for type I error.

In addition, the interdependence between the metal and metalloid content in simultaneous PM_{10} and bulk atmospheric deposition samples was also evaluated at the ETSIIT and CROS sites. The metal and metalloid content in each deposition sample was compared with the monthly mean concentration in the PM_{10} samples calculated from the daily values corresponding to the same sampling period. This comparison was not performed at the CCV site, due to the short time span of the PM_{10} sampling campaign.

3. Results and discussion

3.1 Metal and metalloid concentrations in PM_{10}.

Table 3 summarizes the mean, median, standard deviation, minimum and maximum values of metal and metalloid concentrations in the PM_{10} samples collected at the ETSIIT, CROS and CCV sites. At the ETSIIT and CROS sites, annual mean values of Ni, Cd, As and Pb were well below the established annual target/limit values (20, 5, 6 and 500 $ng \cdot m^{-3}$, respectively), regulated by Directive 2004/107/EC and Directive 2008/50/EC. At the CCV site, despite that the time span was relatively short (28 consecutive days), Ni, As and Pb concentrations in PM_{10} were low with respect to the annual target/limit values. On the contrary, a mean value of 3.47 $ng \cdot m^{-3}$ was obtained for Cd at the CCV site, finding that almost 30% of the samples were above 5 $ng \cdot m^{-3}$ (i.e the annual target value established in Directive 2004/107/EC) during the sampling period. In this regard, further sampling campaigns with a higher time coverage should be developed at the CCV site in order to verify that annual mean concentrations of Cd are below the annual target value established in Directive 2004/107/EC (i.e. 5 $ng \cdot m^{-3}$) and therefore, Cd exposure does not pose a potential health risk for the population living in this area.

With respect to the non-regulated metals and metalloids evaluated in this study, the highest concentrations were found for Mn, Fe and Zn, which are commonly related to the

Mn alloy industry (Marris et al., 2012; Mbengue et al., 2015). The concentration of these metals was higher at the CCV site, in agreement with the greater proximity of this location to the Mn alloy plant.

Although Mn is not included in the European air quality Directives, the World Health Organization (WHO) establishes an annual mean value of 150 $ng \cdot m^{-3}$ as a guideline. As Table 3 shows, whereas annual Mn level at the ETSIIT site (i.e. 60.8 $ng \cdot m^{-3}$) was below the WHO guideline, the annual Mn concentration at the CROS site (i.e. 231.8 $ng \cdot m^{-3}$) exceeded this recommendation, reaching daily values up to 1279.4 $ng \cdot m^{-3}$. At the CCV site, the maximum Mn daily value was 2061.6 $ng \cdot m^{-3}$ and the monthly mean value reached 721.9 $ng \cdot m^{-3}$ (i.e. more than 4 times the WHO guideline). However, these results should be treated with caution due to the short time span of the sampling campaign carried out at the CCV site. On the other hand, increased Mn concentrations (i.e. mean value of 901.1 $ng \cdot m^{-3}$, maximum daily concentration of 2688.3 $ng \cdot m^{-3}$) were also reported for CCV site during a short campaign conducted in February 2017 (Hernández-Pellón et al., 2018). In this regard, and due to the potential health effects of Mn exposure, mainly linked to neurotoxic disorders and cognitive deficits (Chen et al., 2016; Lucchini et al., 2012), Mn is considered as a metal of special concern in the studied area, mainly in the sites located NNW from the Mn alloy plant, which are directly impacted by the plume emanating from the plant when the prevailing winds of the region are blowing (see Figure 2).

3.2 Metal and metalloid deposition fluxes.

Table 4 shows the sum of the deposition rates of the studied metals and metalloids ($\mu g \cdot m^{-2} \cdot d^{-1}$) at the ETSIIT, CROS and CCV sites. The highest deposition fluxes (water-soluble and insoluble fractions) were found at the CCV and CROS sites (i.e. 11998.9 $\mu g \cdot m^{-2} \cdot d^{-1}$ and 4574.8 $\mu g \cdot m^{-2} \cdot d^{-1}$, respectively) in agreement with the greater proximity of these locations to the main industrial sources (see Figure 1). At the three studied sites, the bulk deposition was dominated by the insoluble fraction, reaching the 76%, 82% and 87% of the total deposition at the ETSIIT, CROS and CCV sites, respectively. Mean pH values at the studied sites ranged from 6.4 to 7.1, these values being comparable to others observed in the Mediterranean area (Pieri et al., 2010).

The metal and metalloid content in the bulk atmospheric deposition samples are presented in Table 5. At the CROS and CCV sites the metal and metalloid fluxes followed a similar order: Mn>>Fe>>Zn>>Cu>Pb>V≈Ni>>Cd>As≈Mo≈Sb. The deposition fluxes for all

metals commonly related to the Mn alloy industry (i.e. Mn, Fe, Zn, Cd and Pb) were significantly higher at the CCV site, which is located only 350 m from the Mn alloy plant. For instance, average Mn and Fe fluxes reached 2745.3 $\mu g \cdot m^{-2} \cdot d^{-1}$and 1600.4 $\mu g \cdot m^{-2} \cdot d^{-1}$, respectively, at the CROS site, and 8881.6 $\mu g \cdot m^{-2} \cdot d^{-1}$ and 2545.4 $\mu g \cdot m^{-2} \cdot d^{-1}$, respectively, at the CCV site. At the ETSIIT site the fluxes followed the order Fe>>Zn>Mn>Cu>Pb>Ni>V>As≈Mo>Cd≈Sb. The mean Mn and Fe deposition fluxes at the ETSIIT site were much lower than those found at the CROS and CCV sites, whereas the mean Zn value was slightly higher than that found at the CROS site (211.4 $ng \cdot m^{-3}$ and 173.3 $ng \cdot m^{-3}$, respectively). This can be explained by the presence of other industrial source of Zn, a non-integrated steel plant, which is located 5 km upwind of the ETSIIT site (see Figure 1). Most of the metal and metalloid deposition fluxes presented in Table 5 are comparable to those obtained in other urban/industrial areas (Amodio et al., 2014; Brown et al., 2006; Castillo et al., 2013b; Huston et al., 2012; Motelay-Massei et al., 2005; Sharma et al., 2008). However, Mn deposition rates are in general much higher in comparison with these studies. In this regard, only Menezes-Filho et al. (2016) reported Mn deposition rates measured in the vicinity of a Mn alloy plant in Simões Filho (Brazil) in the same order of magnitude than those found in the present work.

3.3 Metal and metalloid correlations in PM_{10} and deposition

The Spearman correlation coefficients between the measured metals and metalloids in PM_{10} and also in the atmospheric deposition (bulk and water-soluble and insoluble fractions) were evaluated. As Table 6 shows, strong or moderate correlation coefficients were found in PM_{10} samples between all metals frequently related to the Mn alloy industry (i.e. Mn, Fe, Zn, Cd and Pb) (Marris et al., 2012). This interdependence was, in general, higher for the PM_{10} samples collected at the CROS and CCV sites, located closer to the Mn alloy plant, with the exception of Fe-Zn, which presented the highest correlation coefficient at the ETSIIT site. This could be attributed to the major influence in this site of a non-integrated steel plant (see Figure 1), known as an important source of Zn and Fe (Sylvestre et al., 2017), with respect to the greater number of Fe and Zn sources impacting the CROS and CCV sites (i.e. Mn alloy plant and non-exhaust traffic) (Hernández-Pellón and Fernández-Olmo, 2019).

On the other hand, as can be seen in Table 6, only a few significant correlations between specific metals were found for the bulk, water-soluble and insoluble fractions of the

deposition samples. The interdependence between Mn, Fe, Zn, Cd and Pb increased at the CCV site, in the proximity of the Mn alloy plant.

In addition, as indicated in section 2.4, the relationship between the metal and metalloid content in deposition samples and the monthly mean metal and metalloid concentration in PM_{10} samples corresponding to the same sampling period was evaluated at the ETSIIT and CROS sites. In this regard, at the CROS site only the content of both Mn and Cd in PM_{10} and bulk atmospheric deposition samples presented strong and significant correlation coefficients ($r=0.684$, $p<0.01$ and $r=0.680$, $p<0.01$, respectively). These metals have been previously identified as the main tracers of the Mn alloy plant emissions (Hernández-Pellón and Fernández-Olmo, 2019). On the other hand, at the ETSIIT site, located further from the Mn alloy plant, metals and metalloids did not show any significant correlation between their content in PM_{10} and deposition samples.

3.4. Seasonal variability of metal and metalloid PM_{10} concentrations and bulk deposition fluxes

The seasonal variability of the monthly average precipitation and the metal and metalloid concentrations in PM_{10} samples at the ETSIIT and CROS sites are presented in Figure 3. At the ETSIIT site, the levels of Fe, Zn, Cd, Pb and to a minor extent Mn, were higher in autumn, whereas Mo and Cu presented higher concentrations in summer. The levels of Sb were higher during the cold seasons (i.e. winter and autumn). Nickel and V did not show any remarkable seasonal variability at this site, with their lowest levels in spring and winter, respectively. At the CROS site, the highest concentrations were found in autumn for Mn, Fe, Zn, Cd and Pb. No remarkable seasonal variability was identified for Ni, Cu and Mo. Although V and As concentrations in PM_{10} at the ETSIIT and CROS sites were quite homogeneous throughout the year, the lowest levels were identified in winter and autumn, respectively.

The major metal and metalloid sources in the Santander Bay are related to the emissions from the Mn alloy plant and to non-exhaust traffic emissions (Arruti et al., 2011), the former being the major source of metals and metalloids in the southern part of the Bay (e.g. CROS and CCV sites) (Hernández-Pellón and Fernández-Olmo, 2019). In addition, other sources such as a steel-making plant and combustion processes were previously identified, especially impacting the northern part of the Bay (e.g. ETSIIT site) (Arruti et al., 2011). Although the emissions from the Mn alloy plant are expected to be quite

326 homogeneous throughout the year, the highest concentrations in PM_{10} samples of all
327 metals related to the Mn alloy plant emissions (i.e. Mn, Fe, Zn, Cd and Pb) were found in
328 autumn at both ETSIIT and CROS sites, as can be observed in Figure 3. In this period of
329 the year, the winds originate mainly from the S-SW direction. Under this scenario, the
330 plume emanating from the Mn alloy plant is directed towards the sampling sites (see
331 Figure 1). Despite the fact that the wind pattern in this region is similar in winter and
332 autumn, the lower metal and metalloid concentrations found in PM_{10} samples collected
333 in winter can be explained due to the greater scavenging effect associated with the higher
334 precipitations registered during this period. In addition, the higher Cu and Mo levels in
335 summer at the ETSIIT site could be attributed to the greater influence of road traffic as a
336 result of increased tourism during this period of the year. Also, the concentrations of V
337 and Ni are quite constant throughout the year, therefore it is likely that ship emissions
338 from the Santander Bay is the major source of these metals instead of residential
339 combustion (Arruti et al., 2011; Hernández-Pellón and Fernández-Olmo, 2019).

340 Figure 4 shows the seasonal variability of the bulk atmospheric deposition of metals and
341 metalloids ($\mu g \cdot m^{-2} \cdot d^{-1}$) and the monthly average precipitation at the ETSIIT, CROS and
342 CCV sites. Less clear seasonal trends were observed for the deposition of most metals
343 and metalloids, in comparison with the seasonal trends identified for their concentrations
344 in PM_{10} samples. The highest bulk deposition fluxes were found in autumn for Mn and
345 Cd at the three studied locations. The rest of the metals and metalloids showed a different
346 trend between sites. At the ETSIIT site, the deposition fluxes of most metals and
347 metalloids were quite homogeneous throughout the year, only Ni presented higher
348 deposition rates in winter. At the CROS site, the deposition fluxes of V and Ni were
349 higher in winter, whereas Mo presented higher deposition rates in summer. The
350 deposition fluxes of Fe, As, Cu, Zn, Sb and Pb were similar throughout the year. At the
351 CCV site, the highest deposition fluxes were found in autumn for Fe, Ni and Zn and in
352 spring for V, As, Mo and Sb. In addition, the deposition of Cu was similar throughout the
353 year, whereas Pb only presented lower deposition rates in winter.

354 Overall, the highest deposition rates of the metals associated with the Mn alloy plant (i.e.
355 Mn, Fe, Zn, Cd and Pb) were found during the cold seasons (i.e. winter and autumn),
356 when the monthly mean precipitations are high and the most frequent winds came from
357 the S-SW direction.

3.5. Spatial variability of the water-soluble metal and metalloid fraction of the atmospheric deposition

Boxplots of the water-soluble fraction of the measured metals in the deposition samples collected at the ETSIIT, CROS and CCV sites are presented in Figure 5. At the ETSIIT site the average water-soluble fractions of the measured metals followed the order Ni (72%) > Zn (62%) > Cu (60%) > Mn (49%) > V (43%) > Pb (24%) > Fe (10%). In addition, the order was Zn (51%) > Sb (50%) > Cd=Ni (47%) > Mo (42%) > V (34%) > As (30%) > Mn (22%) > Cu (21%) > Pb=Fe (7%) at the CROS site and Ni (34%) > Cd (29%) > Zn (26%) > Mn (23%) > Sb (22%) > V (16%) > Cu (11%) > Pb (9%) > Fe (7%) at the CCV site. The water-soluble fraction of Cd, Mo and Sb in the deposition samples collected at the ETSIIT site and of As and Mo in the deposition samples collected at the CCV site was below the MDL.

As can be observed in Figure 5, the water-soluble fraction of most metals increased with distance from the Mn alloy plant. Only Fe presented similar average water-soluble fractions at the three studied sites, with a higher variability between samples at the ETSIIT and CCV sites. A previous study carried out by this research group reported that deposition samples collected at the CCV site were mostly composed of coarse particles (between 19.9 and 24.8 μm of diameter), containing SiMn slags, Mn alloys and Mn ores, attributed to fugitive emissions from the Mn alloy plant (Hernández-Pellón et al., 2017). According to the literature, the solubility of the metals associated with SiMn slags and Mn alloys is expected to be low (Thomassen et al., 2001). In addition, fugitive emissions of coarse particles have low buoyancy (Fulk et al., 2016) and therefore these less soluble particles will be deposited at the closest receptor sites downwind of the source (i.e. the CCV and CROS sites), whereas more soluble particles coming from point sources (i.e. chimneys) will be deposited at longer distances, which can explain the decrease in the water-soluble fraction of most metals in the atmospheric deposition in the proximity of the Mn alloy plant.

In contrast to these results, a general increase in the solubility in simulated lung fluids (SLF)s of Fe, Mn, Cu, Zn, Cd, and Pb was previously found in PM_{10} samples collected at the CCV site, close to the main industrial sources, with respect to the ETSIIT site (Hernández-Pellón et al., 2018). Mbengue et al. (2015) also reported the decrease of the solubility in SLFs of Cd, Mn, Pb, Zn and Cu with distance from the industrial sources in

390 PM_1 samples impacted by metallurgical activities. In this regard, a previous study showed
391 that most of the particles identified in PM_{10} samples collected at the CCV site were
392 attributed to condensation processes at the smelting unit of the Mn alloy plant. These
393 particles were characterized by spherical shapes and small sizes and expected to be highly
394 soluble (Hernández-Pellón et al., 2017). However, as Marris et al. (2012) reported, fine
395 particles emitted by industrial processes may quickly undergo various physicochemical
396 transformations that change particle composition, size and structure, forming
397 agglomerates of metal-bearing particles and other supplementary mixed particles not
398 primarily presented inside the chimneys.

399 The potential hazard to human health of metal-bearing PM_{10} exposure is expected to be
400 higher in the proximity of the Mn alloy plant, where both the metal concentrations in
401 PM_{10} and the metal solubility in SLFs are higher. However, although the bulk deposition
402 fluxes of the metals related to the Mn alloy plant decrease with distance from the
403 industrial source, the water-soluble fraction of these metals tends to increase. Therefore,
404 the transfer of metals from air to aquatic and terrestrial ecosystems, as well the potential
405 hazard to human health due to metal exposure through dust resuspension mechanisms
406 should be also considered at longer distances from the plant and not only in the vicinity
407 of the industrial activity.

408 **4. Conclusions**

409 A study of the PM_{10} levels and deposition fluxes of eleven potentially toxic metals and
410 metalloids was conducted in three urban sites of the Cantabrian region (northern Spain),
411 located at different distances downwind from a Mn alloy plant. The water-soluble and
412 insoluble fractions of V, Mn, Fe, Ni, Cu, Zn, As, Mo, Cd, Sb and Pb were determined in
413 the deposition samples.

414 Among the studied metals and metalloids, the highest levels in PM_{10} and deposition
415 samples were found for Mn, Fe, Zn, Cu and Pb. The levels in PM_{10} samples of those
416 metals related to the Mn alloy plant (i.e. Mn, Fe, Zn and Pb) were higher in autumn, when
417 the most frequent winds came from the S-SW direction and the plume emanating from
418 the Mn alloy plant is directed towards the studied urban sites. Most metals associated with
419 the Mn alloy industry presented higher deposition rates during the cold seasons (i.e.
420 autumn or winter), which were characterized by high monthly average precipitations. The
421 highest bulk deposition fluxes (water-soluble and insoluble fractions) were found in the

proximity of the Mn alloy plant; however, the water-soluble fraction of most metals increased with distance from this plant. The highest water-soluble fractions were found at the site located further from the Mn alloy plant: Ni (72%), Zn (62%), Cu (60%) and Mn (49%). In this regard, the transfer of metals from air to aquatic and terrestrial ecosystems, as well as the potential hazard to human health due to metal exposure through dust resuspension mechanisms, should be considered not only in the vicinity of this industrial activity, but also at longer distances.

These results will be useful for the health risk assessment of the metal exposure associated with Mn alloy plants, as well as for the evaluation of the metal burden to soil, water and ecosystems related to this industry.

Acknowledgements

This work was financially supported by the Spanish Ministry of Economy and Competitiveness (MINECO) through the CTM2013-43904R Project. Ana Hernández-Pellón would like to thank the Ministry of Economy and Competitiveness (MINECO) for the FPI grant awarded, reference numbers BES-2014-068790.

References

Aas, W., Alleman, L.Y., Bieber, E., Gladtke, D., Houdret, J.L., Karlsson, V., Monies, C., 2009. Comparison of methods for measuring atmospheric deposition of arsenic, cadmium, nickel and lead. J. Environ. Monit. 11(6), 1276-1283. doi:10.1039/b822330k

Al Ali, S., Debade, X., Chebbo, G., Béchet, B., Bonhomme C., 2017. Contribution of atmospheric dry deposition to stormwater loads for PAHs and trace metals in a small and highly trafficked urban road catchment. Environ. Sci. Pollut. Res. Int. 24(34), 26497–26512. doi:10.1007/s11356-017-0238-1

Aljazzar, T., Kocher, B., 2016. Monitoring of contaminant input into roadside soil from road runoff and airborne deposition. Transp. Res. Procedia 14, 2714–2723. doi:10.1016/j.trpro.2016.05.451

Amato, F., Cassee, F.R., Denier van der Gon H.A., Gehrig, R., Gustafsson, M., Hafner,

W., Harrison, R.M., Jozwicka, M., Kelly, F.J., Moreno, T., Prevot, A.S., Schaap, M., Sunyer, J., Querol, X., 2014. Urban air quality : The challenge of traffic non-exhaust emissions. J. Hazard. Mater. 275, 31–36. doi:10.1016/j.jhazmat.2014.04.053

Amodio, M., De Gennaro, G., Di Gilio, A., Tutino, M., 2014. Monitoring of the deposition of PAHs and metals produced by a steel plant in Taranto (Italy). Adv. Meteorol. 2014, 598301. doi:10.1155/2014/598301

Antisari, L.V., Orsini, F., Marchetti, L., Vianello, G., Gianquinto, G., 2015. Heavy metal accumulation in vegetables grown in urban gardens. Agron. Sustain. Dev. 35(3), 1139–1147. doi:10.1007/s13593-015-0308-z

Arruti, A., Fernández-Olmo, I., Irabien, A., 2011. Regional evaluation of particulate matter composition in an atlantic coastal area (Cantabria region, northern Spain): Spatial variations in different urban and rural environments. Atmos. Res., 101(1-2), 280-293. doi:10.1016/j.atmosres.2011.03.001

Bermudez, G.M., Jasan, R., Plá, R., Pignata, M.L., 2012. Heavy metals and trace elements in atmospheric fall-out: Their relationship with topsoil and wheat element composition. J. Hazard. Mater. 213–214:447–456. doi:10.1016/j.jhazmat.2012.02.023

Borgese, L., Federici, S., Zacco, A., Gianoncelli, A., Rizzo, L., Smith, D.R., Donna, F., Lucchini, R., Depero, L.E., Bontempi, E., 2013. Metal fractionation in soils and assessment of environmental contamination in Vallecamonica, Italy. Environ. Sci. Pollut. Res. Int. 20(7), 5067–5075. doi:10.1007/s11356-013-1473-8

Boudissa, S.M., Lambert, J., Müller, C., Kennedy, G., Gareau, L., Zayed, J., 2006. Manganese concentrations in the soil and air in the vicinity of a closed manganese alloy production plant. Sci. Total Environ. 361(1-3), 67–72. doi:10.1016/j.scitotenv.2005.05.001

Bourliva, A., Kantiranis, N., Papadopoulou, L., Aidona, E., Christophoridis, C., Kollias, P., Evgenakis M., Fytianos K., 2018. Seasonal and spatial variations of magnetic susceptibility and potentially toxic elements (PTEs) in road dusts of Thessaloniki city, Greece: A one-year monitoring period. Sci. Total Environ. 639, 417–427. doi:10.1016/j.scitotenv.2018.05.170

Brown, R. J. C., Shaw, M. C., Roberts, M. R., 2006. Practical methodology for the solubility speciation analysis of ambient dust deposits for heavy metals: Application to a 6-month measurement campaign. Int. J. Environ. Anal. Chem. , 86(6), 453-460. doi:10.1080/03067310500291627

Carter, M.R., Gaudet, B.J., Stauffer, D.R., White, T.S., Brantley, S.L., 2015. Using soil records with atmospheric dispersion modeling to investigate the effects of clean air regulations on 60 years of manganese deposition in Marietta, Ohio (USA). Sci. Total Environ. 515–516: 49–59. doi:10.1016/j.scitotenv.2015.01.015

Castillo, S., de la Rosa, J.D., Sánchez de la Campa, A.M., González-Castanedo, Y., Fernández-Caliani, J.C., Gonzalez, I., Romero, A., 2013a. Contribution of mine wastes to atmospheric metal deposition in the surrounding area of an abandoned heavily polluted mining district (Rio Tinto mines, Spain). Sci. Total Environ. 449, 363–372. doi:10.1016/j.scitotenv.2013.01.076

Castillo, S., De la Rosa, J.D., Sánchez de la Campa, A.M., González-Castanedo, Y., Fernández-Camacho, R., 2013b. Heavy metal deposition fluxes affecting an Atlantic coastal area in the southwest of Spain. Atmos. Environ. 77, 509–517. doi:10.1016/j.atmosenv.2013.05.046

Chen, P., Culbreth, M., Aschner, M., 2016. Exposure, epidemiology, and mechanism of the environmental toxicant manganese. Environ. Sci. Pollut. Res. 23(14), 13802–13810. doi:10.1007/s11356-016-6687-0

Child, A.W., Moore, B.C., Vervoort, J.D., Beutel, M.W., 2018. Tracking long-distance atmospheric deposition of trace metal emissions from smelters in the upper Columbia River valley using Pb isotope analysis of lake sediments. Environ. Sci. Pollut. Res. 25(6), 5501–5513. doi:10.1007/s11356-017-0914-1

Connan, O., Maro, D., Hébert, D., Roupsard, P., Goujon, R., Letellier, B., Le Cavelier, S., 2013. Wet and dry deposition of particles associated metals (Cd, Pb, Zn, Ni, Hg) in a rural wetland site, Marais Vernier, France. Atmos. Environ. 67, 394–403. doi:10.1016/j.atmosenv.2012.11.029

Coufalík, P., Mikuška, P., Matoušek, T., Večeřa, Z., 2016. Determination of the bioaccessible fraction of metals in urban aerosol using simulated lung fluids. Atmos.

Environ. 140, 469–475. doi:10.1016/j.atmosenv.2016.06.031

Davidson, C. I., Phalen, R. F., Solomon, P. A., 2005. Airborne particulate matter and human health: A review. Aerosol Sci. Technol., 39(8), 737-749. doi:10.1080/02786820500191348

Davis, B.S., Birch, G.F., 2011. Spatial Distribution of Bulk Atmospheric Deposition of Heavy Metals in Metropolitan Sydney, Australia. Water Soil Air Pollut. 214(1-4), 147–162. doi:10.1007/s11270-010-0411-3

Engels, S., Fong, L.S.R.Z., Chen, Q., Leng, M.J., Mcgowan, S., Idris, M., Rose, N.L., Ruslan, M.S., Taylor, D., Yang, H., 2018. Historical atmospheric pollution trends in Southeast Asia inferred from lake sediment records. Environ. Pollut. 235, 907–917. doi:10.1016/j.envpol.2018.01.007

Fedorová, E., Hančuľák, J., Kurbel, T., Šestinová, O., Findoráková, L., Špaldon, T., 2015. Influence of atmospheric deposition on the selected areas of eastern slovakia-kosice and Krompachy. Procedia Earth Planet. Sci. 15, 833–838. doi:10.1016/j.proeps.2015.08.133

Ferri, R., Hashim, D., Smith, D.R., Guazzetti, S., Donna, F., Ferretti, E., Curatolo, M., Moneta, C., Maria, G., Beone, G.M., Lucchini, R.G., 2015. Metal contamination of home garden soils and cultivated vegetables in the province of Brescia, Italy: Implications for human exposure. Sci. Total Environ. 518–519, 507–517. doi:10.1016/j.scitotenv.2015.02.072

Fiordelisi, A., Piscitelli, P., Trimarco, B., Coscioni, E., Iaccarino, G., Sorriento, D., 2017. The mechanisms of air pollution and particulate matter in cardiovascular diseases. Heart Fail. Rev. 22, 337–347. doi:10.1007/s10741-017-9606-7

Folens, K., van Labeke, M.-C., Dulang, G., 2017. Impact of an Urban Environment on Trace Element Concentrations in Domestically Produced Lettuce (Lactuca sativa L.). Water Air Soil Poll. 228(12),457. doi:10.1007/s11270-017-3635-7

Fomba, K.W., van Pinxteren, D., Müller, K., Spindler, G., Herrmann, H., 2018. Assessment of trace metal levels in size-resolved particulate matter in the area of Leipzig. Atmos. Environ. 176, 60–70. doi:10.1016/j.atmosenv.2017.12.024

541 Fulk, F., Haynes, E.N., Hilbert, T.J., Brown, D., Petersen, D., Reponen, T., 2016.
542 Comparison of stationary and personal air sampling with an air dispersion model for
543 children's ambient exposure to manganese. J. Expo. Sci. Environ. Epidemiol. 26(5),
544 494–502. doi:10.1038/jes.2016.30

545 Guo, L., Lyu, Y., Yang, Y., 2017. Concentrations and chemical forms of heavy metals in
546 the bulk atmospheric deposition of Beijing, China. Environ. Sci. Pollut. Res. 24(35),
547 27356–27365. doi:10.1007/s11356-017-0324-4

548 Hančuľák, J., Fedorová, E., Šestinová, O., Špaldon, T., Matik, M., 2011. Influence of iron
549 ore works in Nižná Slaná on the atmospheric deposition of heavy metals. Acta.
550 Montan. Slovaca. 16(3), 220–228.

551 Hernández-Pellón, A., Fernández-Olmo, I., 2019. Using multi-site data to apportion PM-
552 bound metal(loid)s: Impact of a manganese alloy plant in an urban area. Sci. Total
553 Environ. 651, 1476-1488. doi:10.1016/j.scitotenv.2018.09.261

554 Hernández-Pellón, A., Nischkauer, W., Limbeck, A., Fernández-Olmo, I., 2018.
555 Metal(loid) bioaccessibility and inhalation risk assessment: A comparison between
556 an urban and an industrial area. Environ. Res. 165, 140–149.
557 doi:10.1016/j.envres.2018.04.014

558 Hernández-Pellón, A., Fernández-Olmo, I., Ledoux, F., Courcot, L., Courcot, D., 2017.
559 Characterization of manganese-bearing particles in the vicinities of a manganese
560 alloy plant. Chemosphere 175, 411–424. doi:10.1016/j.chemosphere.2017.02.056

561 Hoek, G., Krishnan, R.M., Beelen, R., Peters, A., Ostro, B., Brunekreef, B., Kaufman,
562 J.D., 2013. Long-term air pollution exposure and cardio- respiratory mortality: A
563 review. Environ. Heal. 12(1), 43. doi:10.1186/1476-069X-12-43

564 Holm, S., 1979. A simple sequentially rejective multiple test procedure. *Scand. J. Stat.*
565 6, 65–70.

566 Hovmand, M.F., Kemp, K., Kystol, J., Johnsen, I., Riis-Nielsen, T., Pacyna, J.M., 2008.
567 Atmospheric heavy metal deposition accumulated in rural forest soils of southern
568 Scandinavia. Environ. Pollut. 155(3), 537-541. doi:10.1016/j.envpol.2008.01.047

569 Huston, R., Chan, Y.C., Chapman, H., Gardner, T., Shaw, G., 2012. Source

apportionment of heavy metals and ionic contaminants in rainwater tanks in a subtropical urban area in Australia. Water Res., 46(4), 1121-1132. doi:10.1016/j.watres.2011.12.008

International Agency for Research on Cancer (IARC), 2016. IARC Monographs on the Evaluation of Carcinogenic Risks to Humans. Outdoor air pollution. Volume 109.

Kelly, F.J., Fussell, J.C., 2012. Size, source and chemical composition as determinants of toxicity attributable to ambient particulate matter. Atmos. Environ. 60, 504–526. doi:10.1016/j.atmosenv.2012.06.039

Liang, J., Fang, H., Wu, L., Zhang, T., Wang, X., 2016. Characterization , Distribution , and Source Analysis of Metals and Polycyclic Aromatic Hydrocarbons (PAHs) of Atmospheric Bulk Deposition in Shanghai, China. Water Air Soil Pollut. 227(7), 234. doi:10.1007/s11270-016-2921-0

Lintern, A., Leahy, P.J., Heijnis, H., Zawadzki, A., Gadd, P., Jacobsen, G., Deletic, A., Mccarthy, D.T., 2016. Identifying heavy metal levels in historical flood water deposits using sediment cores. Water Res. 105, 34–46. doi:10.1016/j.watres.2016.08.041

Lucas, E.L., Bertrand, P., Guazzetti, S., Donna, F., Peli, M., Jursa, T.P., Lucchini, R., Smith, D.R., 2015. Impact of ferromanganese alloy plants on household dust manganese levels: Implications for childhood exposure. Environ. Res. 138, 279–290. doi:10.1016/j.envres.2015.01.019

Lucchini, R.G., Guazzetti, S., Zoni, S., Donna, F., Peter, S., Zacco, A., Salmistraro, M., Bontempi, E., Zimmerman, N.J., Smith, D.R., 2012. Tremor, olfactory and motor changes in Italian adolescents exposed to historical ferro-manganese emission. Neurotoxicology 33(4), 687–696. doi:10.1016/j.neuro.2012.01.005

Marris, H., Deboudt, K., Augustin, P., Flament, P., Blond, F., Fiani, E., Fourmentin, M., Delbarre, H., 2012. Fast changes in chemical composition and size distribution of fine particles during the near-field transport of industrial plumes. Sci. Total Environ. 427–428, 126–138. doi:10.1016/j.scitotenv.2012.03.068

Marrugo-Negrete, J.L., Urango-Cardenas, I.D., Núñez, S.M.B., Díez, S., 2014. Atmospheric deposition of heavy metals in the mining area of the San Jorge river

basin, Colombia. Air Qual. Atmos. Health. 7(4), 577–588. doi:10.1007/s11869-014-0260-0

Mbengue, S., Alleman, L.Y., Flament, P., 2017. Metal-bearing fine particle sources in a coastal industrialized environment. Atmos. Res. 183, 202-211. doi:10.1016/j.atmosres.2016.12.012

Mbengue, S., Alleman, L.Y., Flament, P., 2015. Bioaccessibility of trace elements in fine and ultrafine atmospheric particles in an industrial environment. Environ. Geochem. Health 37 (5), 875–889. http://dx.doi.org/10.1007/s10653-015-9756-2.

Menezes-Filho, J.A., Souza, K.O.F., Rodrigues, J.L.G., Santos, N.R., Bandeira, M.J., Koin, N.L., Oliveira, S.S.P., Godoy, A.L.P.C., Mergler, D., 2016. Manganese and lead in dust fall accumulation in elementary schools near a ferromanganese alloy plant. Environ. Res. 148, 322–329. doi:10.1016/j.envres.2016.03.041

Moreno, T., Pandolfi, M., Querol, X., Lavín, J., Alastuey, A., Viana, M., Gibbons, W., 2011. Manganese in the urban atmosphere: Identifying anomalous concentrations and sources. Environ. Sci. Pollut. Res. 18, 173–183. doi:10.1007/s11356-010-0353-8

Motelay-Massei, A., Ollivon, D., Tiphagne, K., Garban, B., 2005. Atmospheric bulk deposition of trace metals to the seine river basin, France: Concentrations, sources and evolution from 1988 to 2001 in Paris.Water Air Soil Pollut., 164(1-4), 119-135. doi:10.1007/s11270-005-1659-x

Norouzi, S., Khademi, H., Ayoubi, S., Cano, A. F., Acosta, J. A., 2017. Seasonal and spatial variations in dust deposition rate and concentrations of dust-borne heavy metals, a case study from Isfahan, central Iran. Atmos. Pollut. Res., 8(4), 686-699. doi:10.1016/j.apr.2016.12.015

Omrani, M., Ruban, V., Ruban, G., Lamprea, K., 2017. Assessment of atmospheric trace metal deposition in urban environments using direct and indirect measurement methodology and contributions from wet and dry depositions. Atmos. Environ. 168, 101-111. doi:10.1016/j.atmosenv.2017.08.064

Pan, Y.P., Wang, Y.S., 2015. Atmospheric wet and dry deposition of trace elements at 10 sites in Northern China. Atmos. Chem. Phys. 15, 951-972. doi:10.5194/acp-15-951-

630 2015

631 Pant, P., Harrison, R.M., 2013. Estimation of the contribution of road traffic emissions to
632 particulate matter concentrations from field measurements: A review. Atmos.
633 Environ. 77, 78–97. doi:10.1016/j.atmosenv.2013.04.028

634 Pavilonis, B.T., Lioy, P.J., Guazzetti, S., Bostick, B.C., Donna, F., Peli, M., Zimmerman,
635 N.J., Bertrand, P., Lucas, E., Smith, D.R., Georgopoulos, P.G., Mi, Z., Royce, S.G.,
636 Lucchini, R.G., 2016. Manganese concentrations in soil and settled dust in an area
637 with historic ferroalloy production. J. Expo. Sci. Environ. Epidemiol. 25(4), 443–
638 450. doi:10.1038/jes.2014.70.

639 Percot, S., Ruban, V., Roupsard, P., Maro, D., Millet, M., 2016. A New Method for
640 Assessing the Contribution of Atmospheric Deposition to the Stormwater Runoff
641 Metal Load in a Small Urban Catchment. Water Air Soil Pollut. 227(6), 1-13
642 doi:10.1007/s11270-016-2794-2

643 Pieri, L., Matzneller, P., Gaspari, N., Marotti, I., Dinelli, G., Rossi, P., 2010. Bulk
644 atmospheric deposition in the southern Po Valley (Northern Italy). Water Air Soil
645 Pollut. 210(1-4), 155–169. doi:10.1007/s11270-009-0238-y

646 Qiu, K., Xing, W., Scheckel, K. G., Cheng, Y., Zhao, Z., Ruan, X., Li, L., 2016. Temporal
647 and seasonal variations of As, Cd and Pb atmospheric deposition flux in the vicinity
648 of lead smelters in Jiyuan, China. Atmos. Pollut. Res., 7(1), 170-179.
649 doi:10.1016/j.apr.2015.09.003

650 Raaschou-Nielsen, O., Andersen, Z.J., Beelen, R., Samoli, E., Stafoggia, M., Weinmayr,
651 G., Hoffmann, B., Fischer, P., Nieuwenhuijsen, M.J., Brunekreef, B., Xun, W.W.,
652 Katsouyanni, K., Dimakopoulou, K., Sommar, J., Forsberg, B., Modig, L., Oudin,
653 A., Oftedal, B., Schwarze, P.E., Nafstad, P., De Faire, U., Pedersen, N.L., Östenson,
654 C.G., Fratiglioni, L., Penell, J., Korek, M., Pershagen, G., Eriksen, K.T., Sørensen,
655 M., Tjønneland, A., Ellermann, T., Eeftens, M., Peeters, P.H., Meliefste, K., Wang,
656 M., Bueno-de-Mesquita, B., Key, T.J., de Hoogh, K., Concin, H., Nagel, G., Vilier,
657 A., Grioni, S., Krogh, V., Tsai, M.Y., Ricceri, F., Sacerdote, C., Galassi, C.,
658 Migliore, E., Ranzi, A., Cesaroni, G., Badaloni, C., Forastiere, F., Tamayo, I.,
659 Amiano, P., Dorronsoro, M., Trichopoulou, A., Bamia, C., Vineis, P., Hoek, G.,
660 2013. Air pollution and lung cancer incidence in 17 European cohorts: Prospective

661 analyses from the European Study of Cohorts for Air Pollution Effects (ESCAPE).
662 Lancet Oncol. 14, 813–822. doi:10.1016/S1470-2045(13)70279-1

663 Rossini, P., Matteucci, G., Guerzoni, S., 2010. Atmospheric fall-out of metals around the
664 Murano glass-making district (Venice, Italy). Environ. Sci. Pollut. Res. 17(1), 40–
665 48. doi:10.1007/s11356-009-0122-8

666 Roupsard, P., Amielh, M., Maro, D., Coppalle, A., Branger, H., Connan, O., Laguionie,
667 P., Hebert, D., Talbaut, M., 2013. Measurement in a wind tunnel of dry deposition
668 velocities of submicron aerosol with associated turbulence onto rough and smooth
669 urban surfaces. J. Aerosol Sci. 55, 12–24. doi:10.1016/j.jaerosci.2012.07.006

670 Sharma, R. K., Agrawal, M., Marshall, F. M., 2008. Atmospheric deposition of heavy
671 metals (Cu, Zn, Cd and Pb) in Varanasi city, India. Environ. Monit. Assess., 142(1-
672 3), 269-278. doi:10.1007/s10661-007-9924-7

673 Sylvestre, A., Mizzi, A., Mathiot, S., Masson, F., Jaffrezo, J.L., Dron, J., Mesbah, B.,
674 Wortham, H., Marchand, N., 2017. Comprehensive chemical characterization of
675 industrial PM2.5 from steel industry activities. Atmos. Environ. 152, 180–190.
676 doi:10.1016/j.atmosenv.2016.12.032

677 Taylor, M.P., 2015. Atmospherically deposited trace metals from bulk mineral
678 concentrate port operations. Sci. Total Environ. 515–516:143–152.
679 doi:10.1016/j.scitotenv.2015.02.010

680 Thomassen, Y., Ellingsen, D.G., Hetland, S., Sand, G., 2001. Chemical speciation and
681 sequential extraction of Mn in workroom aerosols: analytical methodology and
682 results from a field study in Mn alloy plants. J. Environ. Monit. 3(6), 555–559.
683 doi:10.1039/b104479f

684 Thorpe, A., Harrison, R.M., 2008. Sources and properties of non-exhaust particulate
685 matter from road traffic : A review. Sci. Total Environ. 400, 270–282.
686 doi:10.1016/j.scitotenv.2008.06.007

687 Tositti, L., Pieri, L., Brattich, E., Parmeggiani, S., Ventura, F., 2018. Chemical
688 characteristics of atmospheric bulk deposition in a semi-rural area of the Po Valley
689 (Italy). J. Atmos. Chem. 75(1), 97–121. doi:10.1007/s10874-017-9365-9

690 Venturini, E., Vassura, I., Ferroni, L., Raffo, S., Passarini, F., Beddows, D.C., Harrison,
691 R.M., 2013. Bulk deposition close to a Municipal Solid Waste incinerator : One
692 source among many. Sci. Total Environ. 456–457:392–403.
693 doi:10.1016/j.scitotenv.2013.03.097

694 Wang, Y., Xiong, L., Tang, M., 2017. Toxicity of inhaled particulate matter on the central
695 nervous system: neuroinflammation, neuropsychological effects and
696 neurodegenerative disease. J. Appl. Toxicol. 37, 644–667. doi:10.1002/jat.3451

697

698 Table 1. Operating conditions of the ICP-MS instrument

ICP-MS	Agilent 7500
Plasma power	1500 W
RF Matching	1.92 V
Sample depth	7.5 mm
Torch horizontal	-1 mm
Torch vertical	0 mm
Carrier gas	0.9 L min^{-1}
Makeup gas	0.1 L min^{-1}
S/C Temperature	2 ºC
Nebulizer pump	0.1 rps
He gas flow rate	4 L min^{-1}
Oxide ratio (156/140)	<2%
Doubly charged (70/140)	<2%
Measured isotopes in reaction mode	^{51}V, ^{55}Mn, ^{56}Fe, ^{60}Ni, ^{63}Cu, ^{75}As, ^{66}Zn, ^{95}Mo, ^{111}Cd, ^{121}Sb, ^{207}Pb
Internal standards	^{89}Y, ^{103}Rh, ^{185}Re

699

700

701

Table 2. Metal and metalloid recovery (%) obtained for SRM 1648a and detection limits ($ng \cdot m^{-3}$) calculated for the determination of the total metal and metalloid content in PM_{10} and bulk atmospheric deposition samples.

Element	Recovery (%)	Detection limit ($ng \cdot m^{-3}$)	Detection limit ($ng \cdot m^{-3}$)	Detection limit ($\mu g \cdot m^{-2} \cdot d^{-1}$)
	SRM 1648a	Quartz fiber filters 150 mm	Quartz fiber filters 47 mm	Nitrocellulose filters
V	82±3	0.04	0.03	0.01
Mn	90±4	0.51	2.2	0.17
Fe	87±4	35.4	43.7	0.35
Ni	91±7	1.1	2.1	0.06
Cu	90±4	0.73	0.48	0.02
Zn	82±7	19.5	51.6	0.41
As	86±7	0.25	0.01	0.001
Mo	n.a.	0.15	0.4	0.003
Cd	91±4	0.02	0.01	0.0004
Sb	72±8	0.20	0.08	0.01
Pb	92±6	0.44	0.26	0.22

n.a.: certificated value not available for the reference material (SRM 1648a)

706 Table 3. Metal and metalloid levels ($ng \cdot m^{-3}$) in PM_{10} samples: ETSIIT, CROS and CCV sites.

Element	ETSIIT site[a]					CROS site[b]					CCV site[c]				
	Mean	Median	SD	Min	Max	Mean	Median	SD	Min	Max	Mean	Median	SD	Min	Max
V	1.82	1.59	1.34	0.21	6.20	1.12	0.97	0.83	0.24	4.27	1.69	1.47	0.95	0.61	4.41
Mn	60.8	24.8	89.3	1.79	398.6	231.8	82.2	308.7	5.86	1279.4	721.9	559.4	654.1	11.3	2061.6
Fe	242.9	149.8	336.1	41.3	2078.8	279.4	216.7	225.5	46.2	1017.7	322.0	290.4	192.8	46.8	714.0
Ni	0.96	1.6	0.70	<l.d.	2.94	1.11	1.96	1.33	1.13	7.12	1.39	2.83	0.77	<l.d.	3.65
Cu	15.7	11.3	22.8	1.70	169.3	14.4	19.6	9.24	8.86	27.6	8.83	7.51	3.83	2.72	16.1
Zn	103.8	78.3	97.0	19.7	500.7	127.9	103.9	104.5	27.6	621.4	198.6	178.7	145.0	<l.d.	602.3
As	0.51	1.25	0.57	<l.d.	1.88	0.44	0.14	0.57	<l.d.	1.83	0.38	0.35	0.18	0.14	0.73
Mo	0.78	0.58	0.98	0.17	6.38	1.03	0.97	0.49	0.27	2.38	0.83	0.84	2.05	<l.d.	11.1
Cd	0.45	0.20	0.77	<l.d.	3.77	1.16	0.28	1.99	<l.d.	8.96	3.47	2.11	3.51	0.11	13.1
Sb	0.27	0.33	0.26	<l.d.	1.34	0.41	0.57	0.33	<l.d.	1.20	0.68	0.72	0.37	0.14	1.32
Pb	15.6	8.14	27.2	0.86	177.6	6.91	7.10	6.88	0.53	23.15	44.8	30.1	38.6	0.35	125.9

707 [a] January 2015 – January 2016. 56 daily samples.
708 [b] January 2015 – January 2016. 52 daily samples.
709 [c] September 2015. 28 daily samples.
710

711 Table 4. Mean bulk deposition fluxes ($\mu g \cdot m^{-2} \cdot d^{-1}$) and accumulated precipitation (mm) at the ETSIIT, CROS and CCV sites.

Site	Precipitation (mm)	pH	Total ($\mu g \cdot m^{-2} \cdot d^{-1}$)	Soluble ($\mu g \cdot m^{-2} \cdot d^{-1}$)	Insoluble ($\mu g \cdot m^{-2} \cdot d^{-1}$)
ETSIIT	986.0	6.5±0.7	1099.3	273.1	826.2
CROS	1108.0	7.1±0.6	4574.8	836.3	3738.5
CCV	1079.7	6.4±1.2	11998.9	1576.8	10422.1

712

713

Table 5. Bulk deposition fluxes ($\mu g \cdot m^{-2} \cdot d^{-1}$) of metals and metalloids, both in the water-soluble and insoluble fractions. ETSIIT, CROS and CCV sites.

Element	ETSIIT site[a]					CROS site[b]					CCV site[c]				
	Mean	Median	SD	Min	Max	Mean	Median	SD	Min	Max	Mean	Median	SD	Min	Max
V	1.3	1.2	0.4	0.7	2.1	5.1	4.3	2.9	1.7	12.1	6.3	6.6	2.7	0.8	11.3
Mn	174.0	149.1	107.0	60.5	416.4	2745.3	2853.8	975.2	930.2	4140.1	8881.6	10439.5	5620.3	525.3	16626.7
Fe	697.7	711.7	227.1	373.4	1077.8	1600.4	1565.2	541.6	479.2	2508.8	2545.4	2075.9	2067.2	192.5	6855.5
Ni	3.2	2.0	4.0	1.0	15.4	4.6	3.5	3.5	1.9	14.4	6.2	5.6	4.1	1.3	15.7
Cu	7.5	7.1	2.0	4.7	12.2	27.7	26.2	6.4	20.4	42.6	39.8	45.7	13.1	6.9	53.3
Zn	211.4	161.8	120.2	111.1	543.3	173.3	154.2	58.1	110.2	316.4	475.5	497.4	197.7	60.5	770.2
As	0.2	0.1	0.1	0.1	0.3	0.5	0.5	0.2	0.2	0.9	0.5	0.4	0.4	0.04	1.3
Mo	0.1	0.1	0.02	0.1	0.2	0.6	0.5	0.5	0.3	2.0	0.4	0.5	0.2	0.03	0.8
Cd	0.03	0.01	0.1	<l.d.	0.3	0.9	0.7	0.6	0.3	1.9	3.8	3.7	1.6	0.7	6.5
Sb	0.03	0.02	0.03	<l.d.	0.08	0.4	0.4	0.2	0.3	0.8	0.3	0.4	0.2	0.1	0.7
Pb	3.9	3.3	1.7	2.0	7.8	16.0	13.5	7.6	6.5	36.6	35.4	40.7	17.0	5.4	54.2

[a] January 2015 – January 2016. 12 monthly samples.
[b] January 2015 – January 2016. 12 monthly samples.
[c] September 2015-December 2016. 12 monthly samples.

720 Table 6. Spearman correlation coefficients between the content of metals associated with the manganese alloy plant in PM_{10} and deposition (bulk,
721 water-soluble and water-insoluble) samples at the ETSIIT, the CROS and the CCV sites.

	ETSIIT site				CROS site				CCV site			
	PM_{10}	Deposition			PM_{10}	Deposition			PM_{10}	Deposition		
		Bulk	W-ins	W-sol		Bulk	W-ins	W-sol		Bulk	W-ins	W-sol
N samples	56	12	12	12	52	12	12	12	28	12	12	12
Mn-Fe	**0.55**	0.11	0.23	0.41	**0.61**	0.42	0.22	**0.73**	**0.74**	**0.73**	**0.75**	-0.05
Mn-Zn	**0.55**	0.53	0.18	**0.68**	**0.76**	0.08	0.32	**0.63**	**0.72**	0.55	**0.66**	**0.71**
Mn-Cd	**0.87**	0.48	0.24	n.a.	**0.90**	0.27	**0.62**	0.45	**0.86**	0.38	0.47	**0.70**
Mn-Pb	**0.62**	**0.76**	**0.66**	0.52	**0.84**	0.49	-0.12	**0.66**	**0.83**	0.57	**0.60**	**0.88**
Fe-Zn	**0.76**	**0.76**	0.41	0.41	**0.57**	0.08	0.28	**0.89**	**0.53**	**0.61**	**0.62**	0.42
Fe-Cd	**0.65**	0.04	-0.16	n.a.	**0.59**	0.53	0.16	-0.06	**0.54**	0.41	0.41	0.22
Fe-Pb	**0.62**	0.53	**0.68**	**0.87**	**0.54**	0.34	0.20	**0.74**	**0.59**	0.32	0.34	0.35
Zn-Cd	**0.63**	0.39	0.18	n.a.	**0.80**	0.01	-0.38	-0.06	**0.84**	**0.65**	**0.68**	**0.74**
Zn-Pb	**0.68**	**0.80**	0.21	0.53	**0.71**	**0.62**	0.11	**0.82**	**0.87**	0.44	0.65	**0.78**
Cd-Pb	**0.70**	0.48	0.09	n.a.	**0.91**	0.01	0.34	0.20	**0.93**	**0.81**	**0.87**	**0.85**

722

723 Bulk: Bulk deposition; W-ins: Water-insoluble fraction; W-sol: Water-soluble fraction;

724 In bold caracter correlation is significant at the 0.05 level
725 n.a.: not available
726
727

728 **Figure captions**

729 Figure 1. Sampling sites and main metal and metalloid industrial sources

730 Figure 2. Wind roses during the sampling period at the ETSIIT, CROS and CCV sites.
731 (a) PM_{10} and deposition sampling campaigns at the ETSIIT and CROS sites; (b) PM_{10}
732 sampling campaign at the CCV site; (c) Bulk atmospheric deposition sampling campaign
733 at the CCV site.

734 Figure 3. Seasonal variability of the metal and metalloid levels in PM_{10} ($ng \cdot m^{-3}$) and the
735 average monthly precipitation (mm).

736 Figure 4. Seasonal variability of the bulk atmospheric deposition of metals and metalloids
737 ($\mu g \cdot m^{-2} \cdot d^{-1}$) and the average monthly precipitation (mm).

738 Figure 5. Spatial variability of the water-soluble fractions of the metal deposition (%) at
739 the ETSIIT, CROS and the CCV sites

740

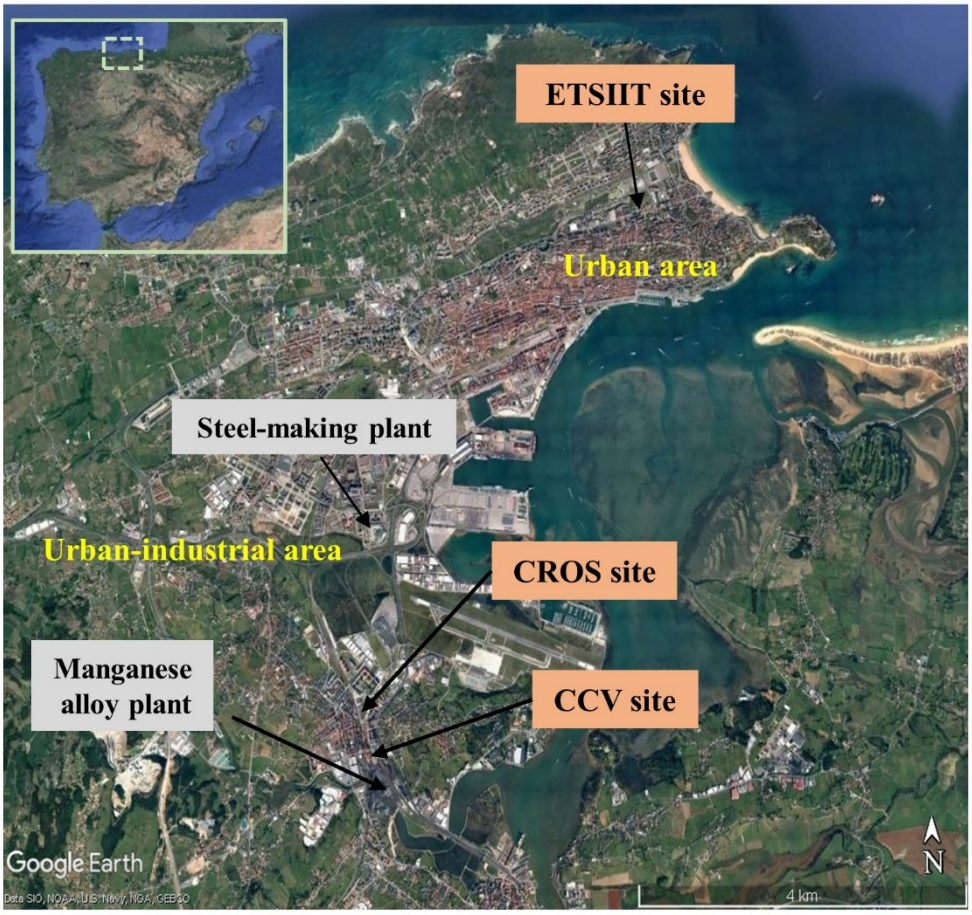

741

742 Figure 1. Sampling sites and main metal and metalloid industrial sources

743

744

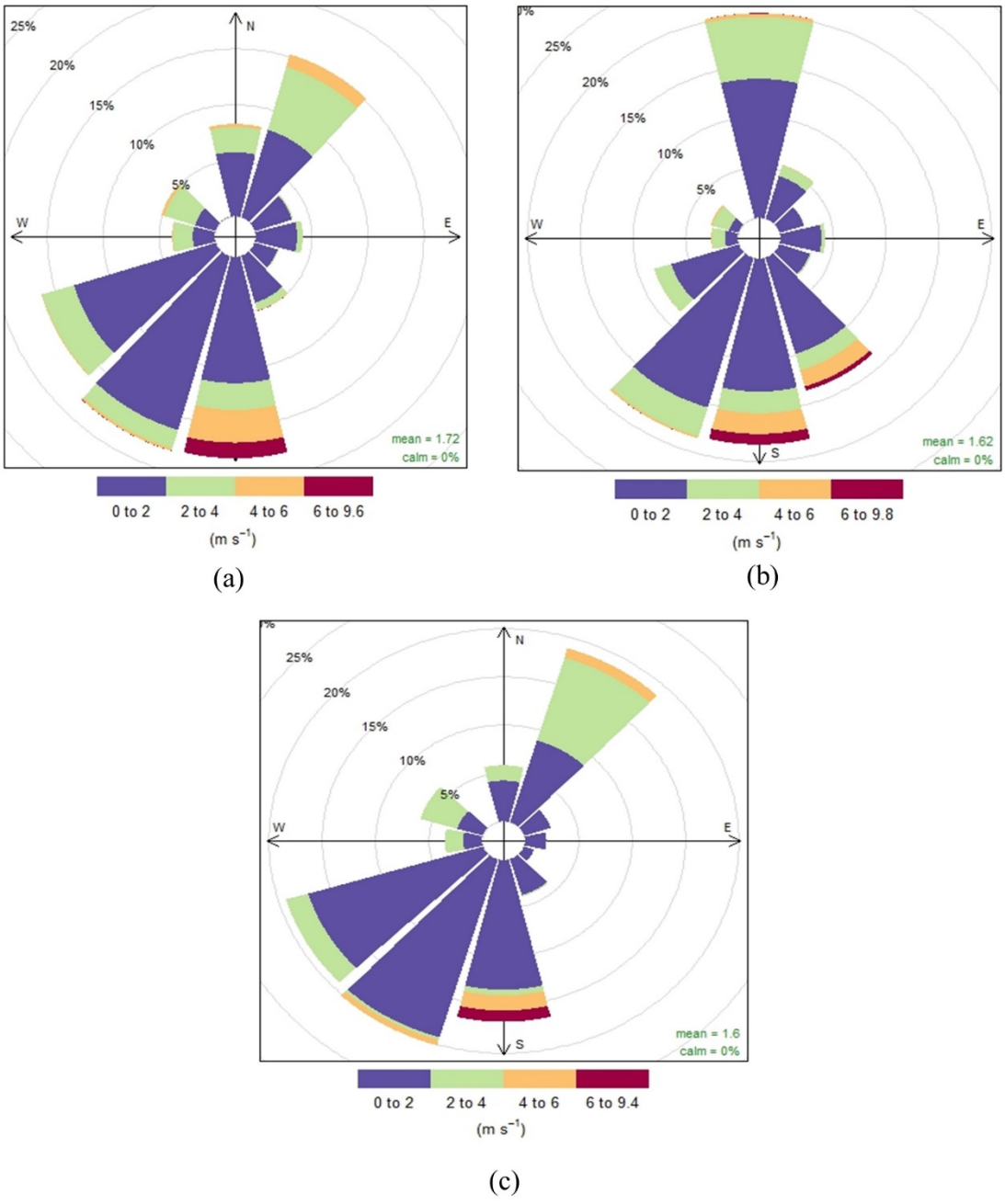

745

746 Figure 2. Wind roses during the sampling period at the ETSIIT, CROS and CCV sites.
747 (a) PM_{10} and deposition sampling campaigns at the ETSIIT and CROS sites; (b) PM_{10}
748 sampling campaign at the CCV site; (c) Bulk atmospheric deposition sampling campaign
749 at the CCV site.

750

751

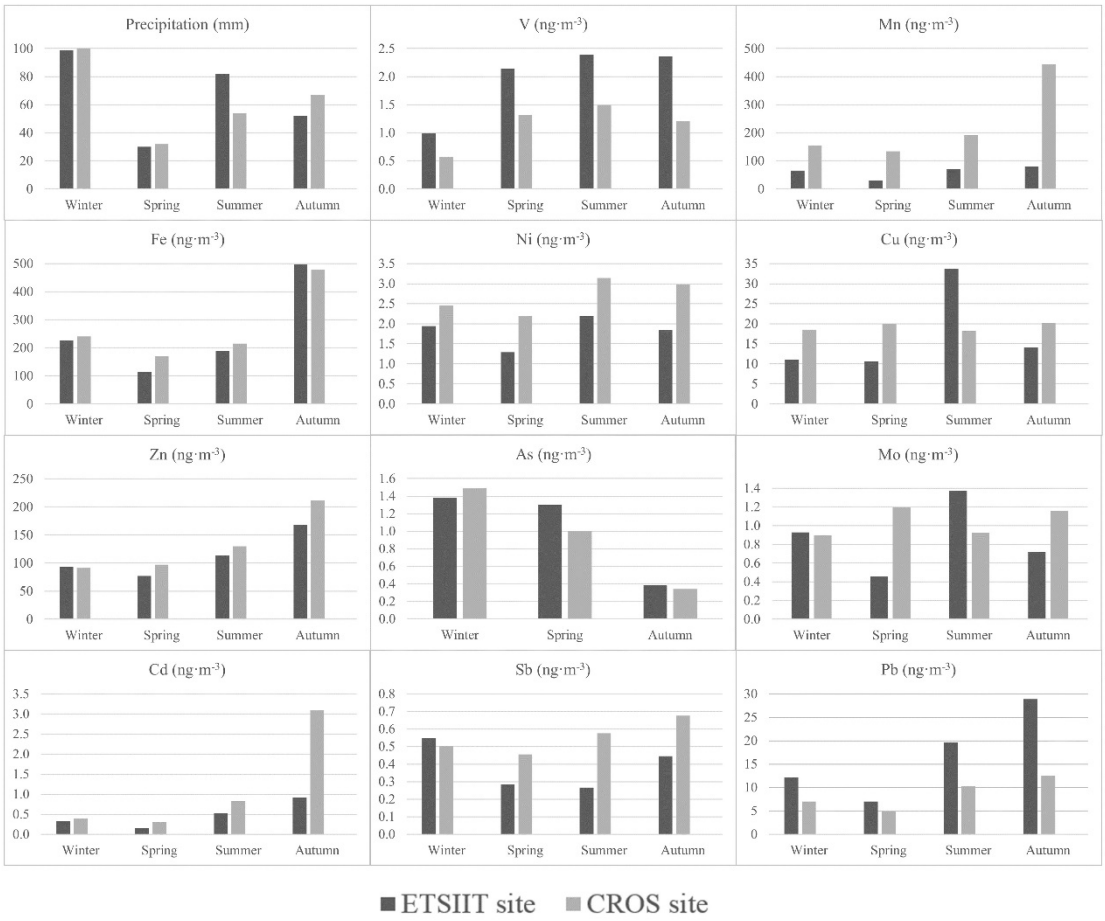

752

753 *As levels in PM_{10} in summer were below the MDL at the ETSIIT and CROS sites

754 Figure 3. Seasonal variability of the metal and metalloid levels in PM_{10} ($ng \cdot m^{-3}$) and the
755 average monthly precipitation (mm).

756

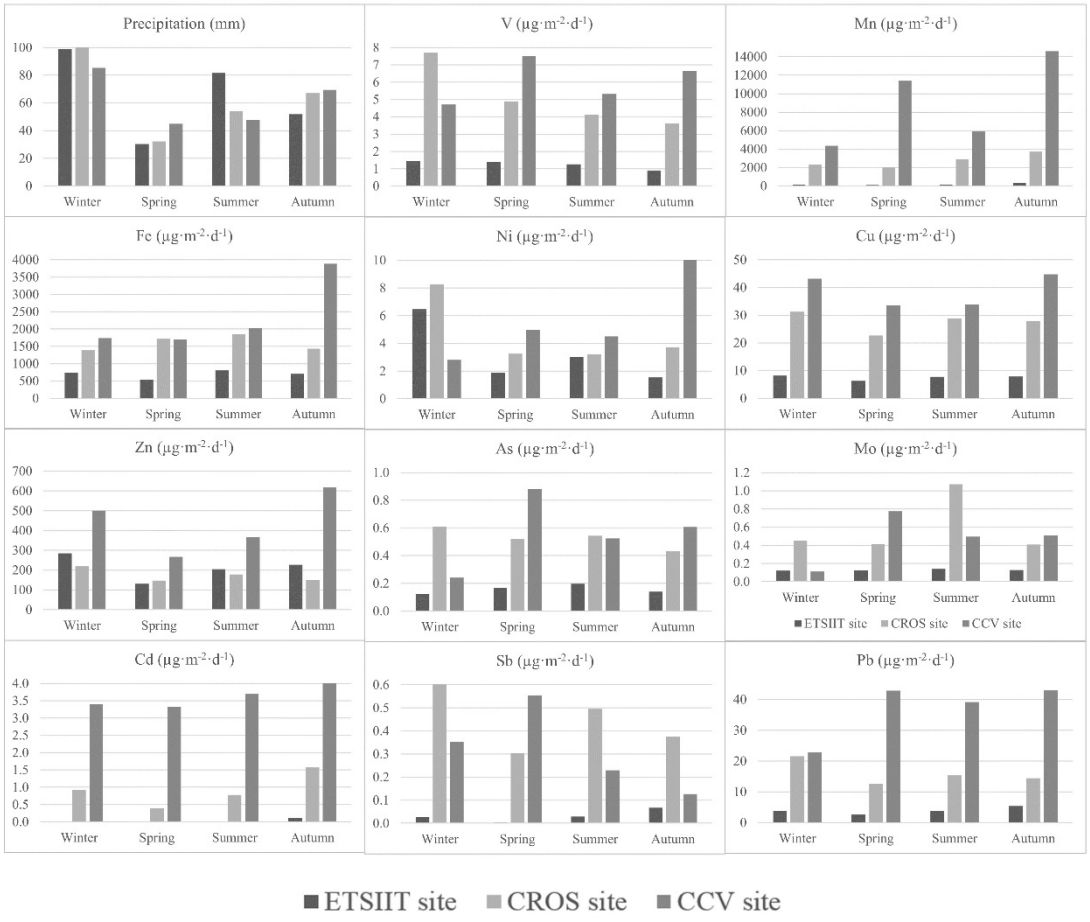

* Mean Cd levels in the bulk atmospheric deposition were below 0.01 µg/m^{2}day in winter, spring and summer at the ETSIIT site

Figure 4. Seasonal variability of the bulk atmospheric deposition of metals and metalloids (µg·m^{-2}·d^{-1}) and the average monthly precipitation (mm).

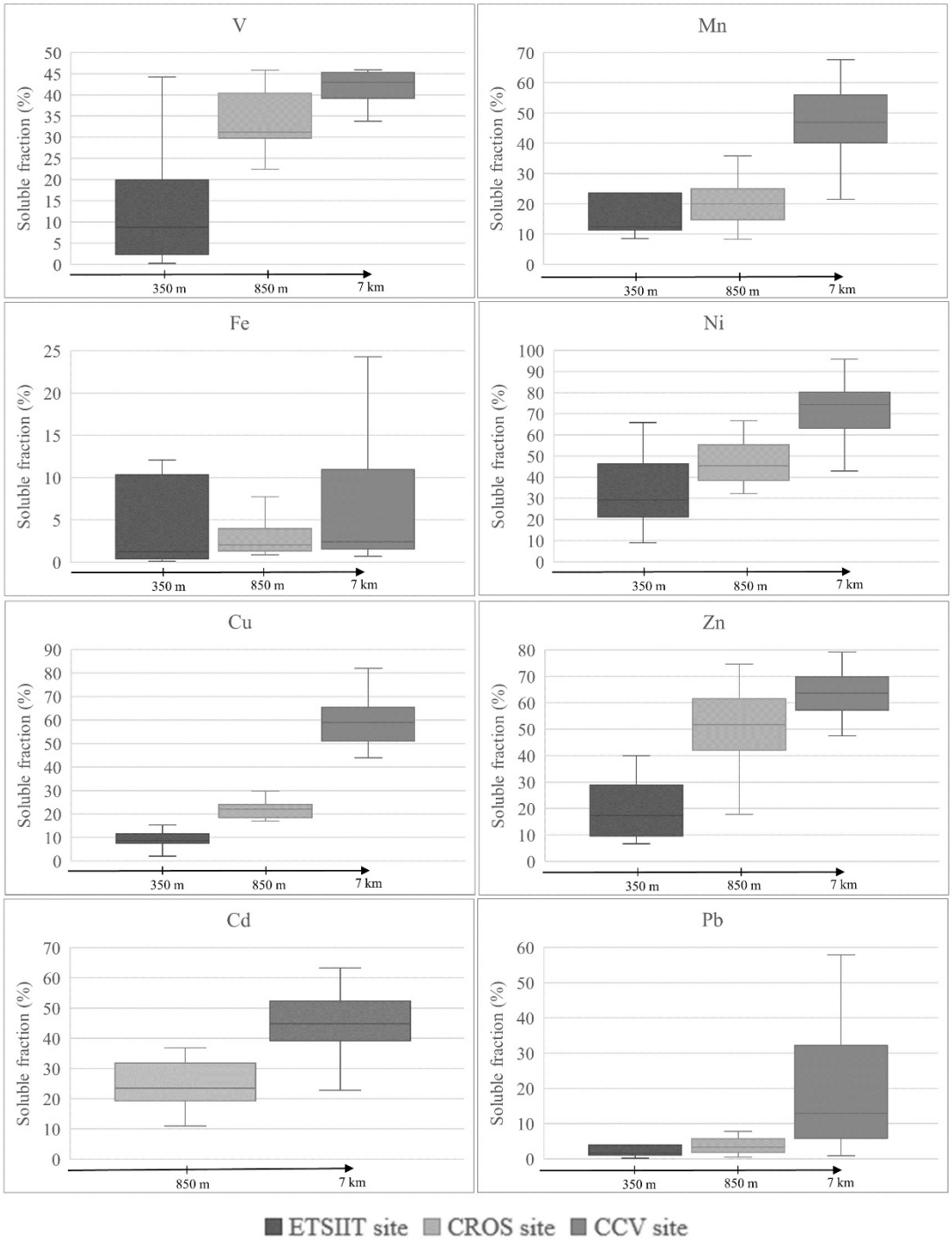

*The water-soluble fraction of Cd in the deposition samples collected at the ETSIIT site was below the MDL.

Figure 5. Spatial variability of the water-soluble fractions of the metal deposition (%) at the ETSIIT, CROS and the CCV sites

Highlights

- Metal and metalloid PM_{10} levels and deposition fluxes were assessed near a Mn alloy plant
- The highest levels in PM_{10} and deposition samples were found for Mn, Fe, Zn, Pb and Cu
- Metal levels in PM_{10} and deposition were higher in autumn and winter
- Metal water-soluble fractions increased with distance from the Mn alloy plant
- Ni (72%), Zn (62%), Cu (60%) and Mn (49%) showed the highest water-soluble fractions

PM_{10}

SAMPLING

- 24-h samples
- 2.3 and 30 $m^3 \cdot h^{-1}$
- 150/47 mm
- Quarz fiber filters

SAMPLE PRETREATMENT

1. Gravimetric determination

2. Acid digestion

HNO_3:H_2O_2 8:2, 220ºC

Refrigerated (4ºC) until analysis

SAMPLING SITES

SANTANDER BAY

METAL ANALYSIS

Water-soluble and insoluble fractions — PM_{10}

UNE14902:2006

ICP-MS

V, Mn, Fe, Ni, Cu, Zn, As, Mo, Cd, Sb, Pb

ATMOSPHERIC DEPOSITION

SAMPLING

- 30± days samples
- Bulk funnel-bottle
- UNE 15841:2016

SAMPLE PRETREATMENT

1. Gravimetric determination

2. Sample filtration

Nitrocellulose filters (47 mm)

Water-soluble	Water-insoluble
50 ml	3. Acid digestion
Acidification with HNO_3	HNO_3:H_2O_2 8:2 220ºC

Refrigerated (4ºC) until analysis